ChemComm

COMMUNICATION

View Article Online
View Journal | View Issue

Cite this: *Chem. Commun.*, 2014, **50**, 2170

Received 23rd November 2013,
Accepted 16th December 2013

DOI: 10.1039/c3cc48948e

www.rsc.org/chemcomm

In situ ^{111}In-doping for achieving biocompatible and non-leachable ^{111}In-labeled Fe_3O_4 nanoparticles†

Jianfeng Zeng,[a] Bing Jia,[b] Ruirui Qiao,[a] Chao Wang,[b] Lihong Jing,[a] Fan Wang[b] and Mingyuan Gao*[a]

The present study reports a new approach for synthesizing ^{111}In-radiolabeled biocompatible Fe_3O_4 nanoparticles. Radioactive ^{111}In is doped *in situ* into the lattice of Fe_3O_4 nanoparticles to achieve robust radiolabeling for accurately tracing PEGylated Fe_3O_4 particles *in vivo*.

Superparamagnetic iron oxide nanoparticles as contrast agents for magnetic resonance imaging (MRI) and platforms for constructing novel molecular imaging probes have been intensively investigated.[1–5] Nevertheless, the pharmacokinetics of iron oxide nanoparticles are rather complex and there remains a lack of in-depth studies. The primary obstacle is accurately tracing the iron oxide particles with the high iron background in tissues. Since radioactive labeling is widely used for evaluating the pharmacokinetics of drugs, labeling iron oxide nanoparticles with radioactive tracers can in principle be adopted for disclosing their pharmacokinetics, in addition to providing novel positron emission tomography (PET)/MRI and single photon emission computed tomography (SPECT)/MRI dual-modality imaging probes.

Towards this goal, iron oxide nanoparticles were radiolabeled with metal radioisotopes (*e.g.*, ^{64}Cu, ^{111}In, and ^{99m}Tc) through chelating ligands.[6–8] However, the chelated radioactive metal ion suffers from heavy leaching *in vivo* due to the transchelation induced by proteins.[9,10] In addition, the ligand detachment from a particle surface also gives rise to dissociation of the radiolabels and provides inaccurate pharmacokinetic information for the labeled nanoparticles.[11] Although labeling the particle surface with a non-metal radioisotope (*e.g.*, ^{125}I and ^{14}C) is an alternative approach to avoid the transchelation, the issues of ligand detachment *in vivo* remain.[3,11]

In contrast to the abovementioned surface radiolabeling methods, incorporating radioisotopes into the iron oxide particle core is expected to be more reliable for tracing the particles *in vivo*. Recently, Louie and coworkers reported ^{64}Cu-doped Fe_3O_4 nanoparticles prepared by co-precipitating Fe^{2+}/Fe^{3+} in the presence of $^{64}Cu^{2+}$ through a microwave-assisted aqueous phase synthesis.[12] The resulting radiolabeled particles were rather polydisperse and irregular in shape. Alternatively, Nielsen and coworkers firstly prepared high quality monodisperse oleate-capped Fe_3O_4 nanoparticles, then achieved radioactive Fe_3O_4 particles through isotopic exchange by incubating the Fe_3O_4 particles with $^{59}FeCl_3$ in chloroform in the presence of free oleic acid.[11] However, after being transferred into TBE buffer by encapsulating the hydrophobic particle with an amphiphilic polymer, the iron oxide particles experienced 3% dissociation of ^{59}Fe after 24 h dialysis.[11] For accurate *in vivo* tracing of Fe_3O_4 nanoparticles, effective suppression of any leaching of the radiolabel is highly preferable. Following on from our previous studies on "one-pot" synthesis of biocompatible Fe_3O_4 nanoparticles,[1,13] herein we report a reliable approach for achieving non-leachable and biocompatible Fe_3O_4 nanoparticles labeled by ^{111}In.

In brief, PEGylated In-doped Fe_3O_4 nanoparticles were prepared by pyrolyzing ferric acetylacetonate ($Fe(acac)_3$) in the presence of indium(III) chloride, α,ω-dicarboxyl-terminated polyethylene glycol (PEG), and oleylamine in diphenyl ether. As shown in Fig. 1, in comparison to the undoped Fe_3O_4 nanoparticles (7.8 ± 1.1 nm), the In : Fe feeding ratio of 1 : 1000 hardly alters the particle size and size distribution, in contrast to those above 1 : 5 as shown in Fig. S1 (ESI†). Powder X-ray diffraction measurements further demonstrate that the undoped nanoparticles are magnetite. Although the samples obtained using different In : Fe feeding ratios exhibit similar diffraction patterns, the peak positions gradually shift to lower angles against the In : Fe ratio, indicating effective incorporation of In^{3+} into the magnetite lattice, since In^{3+} has a larger ionic radius than Fe^{3+}. Taking the dose of 1–20 mg Fe per kg body weight for the *in vivo* imaging applications of Fe_3O_4 nanoparticles into consideration,[1,3–5] a doping level of 1 : 100 000 for ^{111}In : Fe is sufficient. Since approximately 75% of the feeding In^{3+} was incorporated for all feeding ratios, the In-doped Fe_3O_4 particles obtained using an In : Fe ratio of 1 : 1000 were selected for the subsequent experiments and named as 1‰ In-doped Fe_3O_4 nanoparticles.

[a] *Institute of Chemistry, Chinese Academy of Sciences, Bei Yi Jie 2, Zhong Guan Cun, Beijing 100190, China. E-mail: gaomy@iccas.ac.cn; Web: www.gaomingyuan.com; Fax: +86 10 8261 3214*

[b] *Medical Isotopes Research Center, Peking University, Xueyuan Road 38, Beijing 100191, China*

† Electronic supplementary information (ESI) available: (1) Experimental details, (2) characterization of the In-doped and Co-doped Fe_3O_4 nanoparticles, (3) In release experiments, and (4) radioactive decay of intravenously injected ^{111}In-doped Fe_3O_4 nanoparticles. See DOI: 10.1039/c3cc48948e

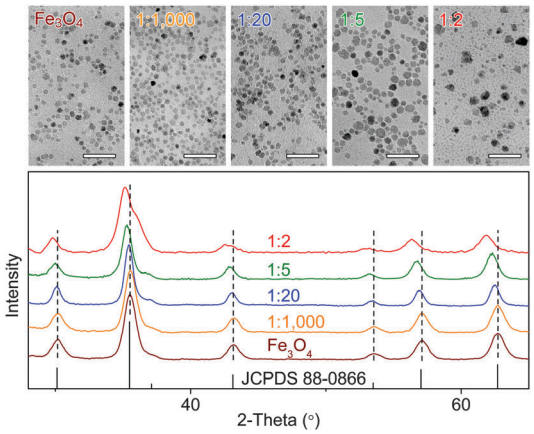

Fig. 1 TEM images (upper panel) and X-ray diffraction patterns (lower panel) of In-doped Fe_3O_4 nanoparticles with different In : Fe feeding ratios.

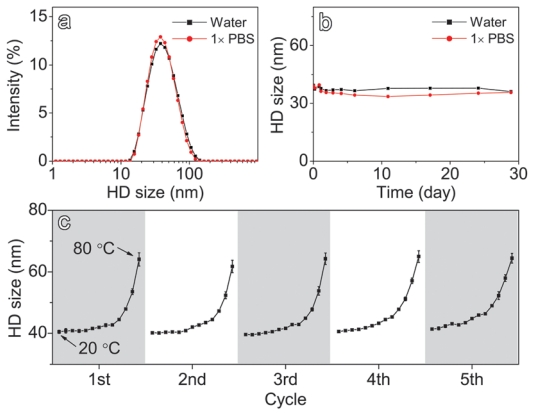

Fig. 2 Hydrodynamic (HD) size profiles (a), temporal evolutions of the hydrodynamic size in water and PBS buffer (b), and temperature-dependent hydrodynamic size of 1‰ indium-doped Fe_3O_4 nanoparticles in water (c).

As colloidal stability under physiological conditions is an important prerequisite for the *in vivo* applications of Fe_3O_4 nanoparticles, the solution properties of the resultant 1‰ In-doped Fe_3O_4 nanoparticles were subjected to careful investigations by dynamic light scattering (DLS). As shown in Fig. 2a, the PEGylated In-doped Fe_3O_4 particles present narrow hydrodynamic size profiles in Milli-Q water and 1× PBS, respectively, with a single scattering peak located at around 37 nm. Long term observations over 30 days demonstrate that 1‰ In-doped Fe_3O_4 nanoparticles possess excellent colloidal stability in both Milli-Q water and PBS buffer at room temperature (Fig. 2b). Further temperature-dependent DLS studies on a PEGylated particle solution, repeatedly subjected to heating up to 80 °C and then cooling down to room temperature for 5 cycles, demonstrate that the In-doped Fe_3O_4 particles exhibit robust colloidal stability through heavy temperature variations, as shown in Fig. 2c.

The leaching properties of the In dopant were studied by inductively coupled plasma mass spectrometry. As shown in Fig. S2 (ESI†), less than 0.03% of the indium was leached from 1‰ In-doped Fe_3O_4 particles over 3 day dialysis against Milli-Q water.

Based on the abovementioned cold indium doping experiments, ^{111}In-doped Fe_3O_4 nanoparticles were prepared in the presence of 10 mCi $^{111}InCl_3$, corresponding to ~10% of the cold indium, for

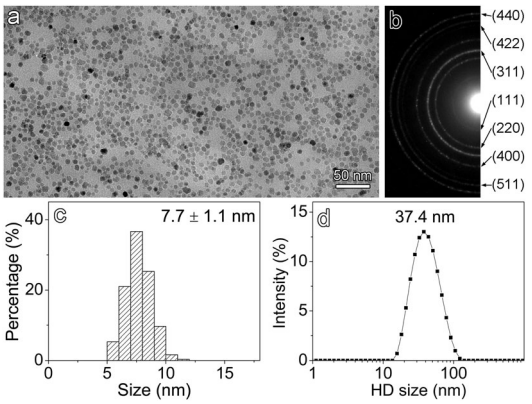

Fig. 3 TEM image (a), selected area electron diffractions identified by lattice planes of magnetite (JCPDS 88-0866) (b), TEM size distribution (c), and hydrodynamic size profile (d) of ^{111}In-doped Fe_3O_4 nanoparticles.

preparing 1‰ ^{111}In-doped Fe_3O_4 nanoparticles. It should be mentioned that the TEM and DLS characterizations carried out after radioactive decay over 400 days, as shown in Fig. 3, suggest that the ^{111}In-doped Fe_3O_4 nanoparticles present nearly no difference in comparison with those obtained by using non-radioactive In as shown in the upper panel of Fig. 1. The average particle size was 7.7 ± 1.1 nm and the hydrodynamic size was 37.4 nm, derived from the single scattering peak.

Using a radioactivity meter in combination with the 1,10-phenanthroline spectrophotometric method for determining the Fe content,[13] the specific activity of the as-prepared ^{111}In-doped Fe_3O_4 nanoparticles was estimated to be 80 μCi per mg Fe. To further investigate the release of ^{111}In, the as-prepared ^{111}In-doped Fe_3O_4 nanoparticles were incubated in Milli-Q water solutions of different pH and 1× PBS buffer, respectively. Through the instant thin-layer chromatography method, the amount of leached ^{111}In was determined. As shown in Fig. 4a, almost no ^{111}In was released at pH higher than 2 over 5-day incubation, while the heavy release at pH lower than 2 is mainly caused by the decomposition of Fe_3O_4 nanoparticles, which further proves that incorporating ^{111}In into the Fe_3O_4 lattice is effective for suppressing the release of the radioactive label. To assess the radiolabeling stability under physiological conditions, ^{111}In-labeled Fe_3O_4 nanoparticles were also incubated in saline and FBS, respectively. The radiolabel in the filtrate and residue obtained by ultrafiltration was determined by a gamma counter. The results shown in Fig. 4b reveal that 0.0059% and 0.0075% of ^{111}In are released in saline and FBS, respectively, after 24 h incubation, several orders of magnitude lower than those (1–10%) reported in the literature for

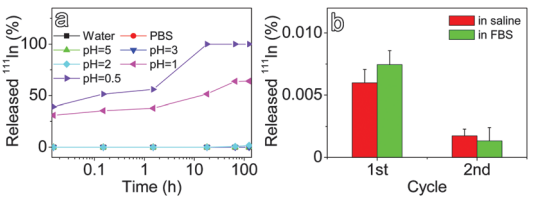

Fig. 4 Leaching properties of ^{111}In-doped Fe_3O_4 nanoparticles in different environments: temporal ^{111}In release in PBS buffer and water solutions with different pH (a) and ^{111}In release in saline and FBS, respectively, after 24 h incubation for 2 cycles (b).

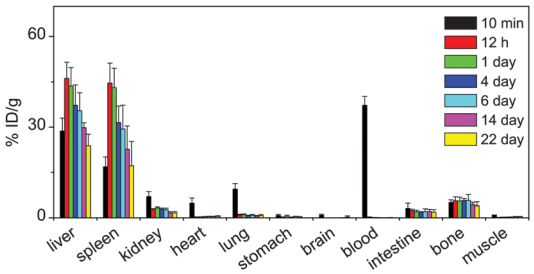

Fig. 5 Biodistribution of ^{111}In-doped Fe_3O_4 nanoparticles in different organs and tissues of mice (n = 5) based on radioactivity measurements by taking the radioactive decay of ^{111}In into consideration.

radiolabeled nanoparticles.[3,7,14] Moreover, almost no ^{111}In is released in the second cycle of incubation, demonstrating that the ^{111}In-doped Fe_3O_4 nanoparticles remain stable under physiological conditions and further suggesting that incorporating the radiolabels into the lattice of the particle matrix is superior to attaching them on the particle surface for achieving stable radiolabeling.

Owing to the excellent radiolabeling stability, ^{111}In-doped Fe_3O_4 nanoparticles were used for revealing the biodistribution of the PEGylated Fe_3O_4 nanoparticles in mice. As shown in Fig. 5, the Fe_3O_4 particles are highly distributed in blood and blood rich organs such as liver, spleen, and lungs, shortly (10 min) after they are delivered through tail vein injection. This is followed by accumulation in the mononuclear phagocyte system (MPS), defined as the cell family of bone marrow progenitors, blood monocytes, and tissue macrophages (such as Kupffer cells in liver and red pulp macrophages in spleen) at prolonged time as is typical,[8,11,14,15] which explains the high distributions of the particles in liver, spleen, and bones. The distributions in kidneys and intestine are probably associated with renal and fecal excretions according to previous studies.[15] This is also supported by the fact that liver and spleen uptake reach the highest values of 46.2% and 44.6% ID per g, 12 h post injection, and then decrease to 23.9% and 17.2% ID per g, respectively, after 22 days. This is much faster than the decay observed for kidneys and intestine. In contrast, organs such as heart, stomach, brain, and muscles exhibit low or negligible particle uptakes.

To further reveal the residence time of the PEGylated Fe_3O_4 nanoparticles, the radioactivity of a group of mice was continually monitored for 250 h after the same dose of ^{111}In-doped Fe_3O_4 nanoparticles was intravenously injected. By fitting the results shown in Fig. S3 (ESI†), the biological half-time of 7.7 nm PEGylated Fe_3O_4 is estimated to be $\sim$33 days.

As a matter of fact, there are limited radiotracers suitable for being incorporated into the lattice of iron oxide nanoparticles. In a parallel attempt, $^{57}Co^{2+}$ was adopted for labeling the PEGylated Fe_3O_4 nanoparticles through pyrolyzing ferric acetylacetonate and cobaltous acetylacetonate using a Co : Fe feeding ratio of 1 : 2 to form $CoFe_2O_4$. Since Co^{2+} has a very similar ionic radius to Fe^{2+}, doping Fe_3O_4 with Co leads to nearly no change in particle size and size distributions, as demonstrated by the results shown in Fig. S4 (ESI†). Nevertheless, the leaching measurement based on inductively coupled plasma atomic emission spectroscopy revealed that cobaltous ions were continuously released from the resultant nanoparticles in aqueous media. Approximately 19.1% of the Co dopant was released after 1 day dialysis against Milli-Q water. Radioactivity measurements revealed that 21.0% of ^{57}Co was released by ^{57}Co-doped $CoFe_2O_4$ nanoparticles after they were dialyzed against Milli-Q water for 1 day. The difference in the dopant leaching behaviors between ^{111}In-doped Fe_3O_4 and ^{57}Co-doped $CoFe_2O_4$ nanoparticles is mainly caused by the huge difference in the solubility product values of the corresponding dopant hydroxides, *i.e.*, 2×10^{-16} for $Co(OH)_2$ and 1.3×10^{-37} for $In(OH)_3$. The low solubility product is apparently in favor of reducing the leaching level of the dopant.

In summary, by pyrolyzing $Fe(acac)_3$ in the presence of carboxylated PEG, oleylamine, and radioactive isotope (^{111}In or ^{57}Co) in diphenyl ether, radiolabeled biocompatible Fe_3O_4 nanoparticles can be obtained. Although both In^{3+} and Co^{2+} can be effectively incorporated into the lattice of Fe_3O_4, ^{111}In-doped Fe_3O_4 nanoparticles present a much lower leaching level than ^{57}Co-doped counterparts. Apart from the excellent anti-leaching properties, the particle surface PEGylation endows the In-doped Fe_3O_4 nanoparticles with excellent colloidal stability under physiological conditions. The ^{111}In label can thus be used to reveal the time-dependent biodistribution of the PEGylated Fe_3O_4 nanoparticles that have previously been demonstrated to be an effective platform for constructing versatile molecular imaging probes. In conclusion, the current investigations have paved a reliable way to achieve non-leachable radiolabeled Fe_3O_4 nanoparticles. Since the specific activity of ^{111}In-radiolabeled nanoparticles can be largely tailored by the doping level, the current method is also suitable for constructing SPECT/MR dual-modality imaging probes.

This work was supported by the National Basic Research Program of China (2011CB935800) and NSFC (81090271, 21003135, 21021003).

Notes and references

1 F. Q. Hu, L. Wei, Z. Zhou, Y. L. Ran, Z. Li and M. Y. Gao, *Adv. Mater.*, 2006, **18**, 2553–2556.
2 J. H. Lee, Y. M. Huh, Y. Jun, J. Seo, J. Jang, H. T. Song, S. Kim, E. J. Cho, H. G. Yoon, J. S. Suh and J. Cheon, *Nat. Med.*, 2007, **13**, 95–99.
3 S. J. Liu, B. Jia, R. R. Qiao, Z. Yang, Z. L. Yu, Z. F. Liu, K. Liu, J. Y. Shi, H. Ouyang, F. Wang and M. Y. Gao, *Mol. Pharmaceutics*, 2009, **6**, 1074–1082.
4 B. H. Kim, N. Lee, H. Kim, K. An, Y. I. Park, Y. Choi, K. Shin, Y. Lee, S. G. Kwon, H. B. Na, J.-G. Park, T.-Y. Ahn, Y.-W. Kim, W. K. Moon, S. H. Choi and T. Hyeon, *J. Am. Chem. Soc.*, 2011, **133**, 12624–12631.
5 R. Qiao, Q. Jia, S. Hüwel, R. Xia, T. Liu, F. Gao, H.-J. Galla and M. Gao, *ACS Nano*, 2012, **6**, 3304–3310.
6 B. R. Jarrett, B. Gustafsson, D. L. Kukis and A. Y. Louie, *Bioconjugate Chem.*, 2008, **19**, 1496–1504.
7 L. Sandiford, A. Phinikaridou, A. Protti, L. K. Meszaros, X. Cui, Y. Yan, G. Frodsham, P. A. Williamson, N. Gaddum, R. M. Botnar, P. J. Blower, M. A. Green and R. T. M. de Rosales, *ACS Nano*, 2013, **7**, 500–512.
8 R. Misri, D. Meier, A. C. Yung, P. Kozlowski and U. O. Hafeli, *Nanomedicine*, 2012, **8**, 1007–1016.
9 L. A. Bass, M. Wang, M. J. Welch and C. J. Anderson, *Bioconjugate Chem.*, 2000, **11**, 527–532.
10 R. M. Reilly, P. Chen, J. Wang, D. Scollard, R. Cameron and K. A. Vallis, *J. Nucl. Med.*, 2006, **47**, 1023–1031.
11 B. Freund, U. I. Tromsdorf, O. T. Bruns, M. Heine, A. Giemsa, A. Bartelt, S. C. Salmen, N. Raabe, J. Heeren, H. Ittrich, R. Reimer, H. Hohenberg, U. Schumacher, H. Weller and P. Nielsen, *ACS Nano*, 2012, **6**, 7318–7325.
12 R. M. Wong, D. A. Gilbert, K. Liu and A. Y. Louie, *ACS Nano*, 2012, **6**, 3461–3467.
13 Q. Jia, J. Zeng, R. Qiao, L. Jing, L. Peng, F. Gu and M. Gao, *J. Am. Chem. Soc.*, 2011, **133**, 19512–19523.
14 C. Glaus, R. Rossin, M. J. Welch and G. Bao, *Bioconjugate Chem.*, 2010, **21**, 715–722.
15 C. Liu, Z. Gao, J. Zeng, Y. Hou, F. Fang, Y. Li, R. Qiao, L. Shen, H. Lei, W. Yang and M. Gao, *ACS Nano*, 2013, **7**, 7227–7240.

